an internal drain-to-channel feedback capacitor. The effect of the capacitor is regenerative, is appreciable at microwave frequencies, and is not changed in nature by the presence of parasitic-source resistance.

ACKNOWLEDGMENT

The author wishes to thank H. Johnson for discussions, and also R. S. Hopkins, W. Baechtold, and C. A. Liechti who generously supplied prepublished data. Advice and encouragement were given by Prof. J. Frey.

REFERENCES

[1] H. Johnson, "A high-frequency representation of the MOS transistor," *Proc. IEEE* (Lett.), vol. 54, pp. 1970–1971, Dec. 1966.
[2] R. S. Hopkins, Jr., "High-frequency Y-parameters of the MOS transistor," Ph.D. dissertation, Rutgers Univ., New Brunswick, N. J., 1970.
[3] W. Baechtold, "Microwave GaAs Schottky-barrier field-effect transistors and their applications in amplifiers," presented at the 4th Biennial Conf. Microwave Semiconductor Devices, Circuits and Applications, Cornell Univ., Ithaca, N. Y., 1973.
[4] W. Fisher, "Equivalent circuit and gain of MOS field-effect transistors," *Solid-State Electron.*, vol. 9, pp. 71–81, 1966.
[5] *RCA Data Sheet*, 3N128 Transistor, Radio Corp. of America, File no. 309.
[6] C. A. Liechti *et al.*, "GaAs microwave Schottky-gate FET," in *Proc. 1972 IEEE Int. Solid State Circuits Conf.*, pp. 158–159.
[7] C. A. Liechti, "Design and performance of microwave amplifiers with GaAs Schottky-gate field-effect transistors," *IEEE Trans. Microwave Theory Tech.*, to be published.
[8] ——, private communication.

Broad-Band Varactor-Tuned IMPATT-Diode Oscillator

DALE H. CLAXTON, MEMBER, IEEE, AND
PAUL T. GREILING, MEMBER, IEEE

***Abstract*—A varactor-tuned IMPATT-diode oscillator with a continuous and monotonic tuning bandwidth of 27 percent and a potential tuning range in excess of 40 percent is described. The results of a computer program which optimizes the tuning bandwidth of the equivalent circuit of the voltage-controlled oscillator (VCO) are presented. The VCO consists of two varactors located symmetrically on each side of an IMPATT diode all mounted in a ridged waveguide with two matched outputs into 50-Ω coaxial. Experimental results on bandwidth, power output, frequency linearity, and FM noise are presented.**

I. INTRODUCTION

Satellite and spacecraft applications have created a need for microwave, solid-state, electronically tuned oscillators which are tunable over a broad frequency range, exhibit high dc-to-RF conversion efficiency, and have low noise properties. Broad tuning range means fewer oscillators are needed for a given receiver bandwidth, and obviates the need for complicated switching schemes. Efficiency is essential for satellite and spacecraft applications, and low noise is a requirement for good receiver sensitivity.

Solid-state devices have been in existence for years which have the capability of meeting these requirements, but have not as yet realized their full potential. The main stumbling block has been that the devices are difficult to impedance match over a broad frequency range. Tunnel diodes are not acceptable for these applications because of their low power levels [1], whereas TRAPATT diode oscillators are inherently narrow band because the fundamental and first several harmonically related frequencies must be matched and tuned simultaneously [2]. Transferred-electron devices (TED's) are ruled out because of system efficiency requirements. The TED's generally operate at less than 5-percent dc-to-RF efficiency, and if YIG tuned, the voltage-controlled oscillator (VCO) efficiency would be less than 1 percent [3].

IMPATT diodes possess all of the characteristics which satisfy the power, efficiency, and broad-band negative resistance requirements. However, because of the circuit problem of broad-band impedance matching, IMPATT diode VCO's have been limited to 10-percent bandwidths [4]–[7]. It is the purpose of this short paper to describe an impedance-matching circuit which theoretically yields a total tuning range in excess of 40 percent and to present experimental results for this circuit configuration which are in excess of 27 percent. This was accomplished without significant sacrifice in power output and efficiency, and with an improvement of 8–10 dB in noise performance over previously reported state-of-the-art results.

This short paper is divided into two parts consisting of the theoretical model of the VCO and the experimental results. A computer program is used to analyze the theoretical model of the VCO which consists of the large-signal admittance of an IMPATT diode and the equivalent circuit of the varactor-loaded microwave circuit. Experimental techniques are described which were used to determine the equivalent-circuit element values. Finally, the overall performance (bandwidth, output power, efficiency, and FM noise) of a VCO is presented.

II. EQUIVALENT CIRCUIT

The equivalent circuit of a voltage-controlled IMPATT-diode oscillator consists of the large-signal circuit model of the diode and the voltage-dependent equivalent circuit of the varactor and microwave circuit. The operation of the oscillator is governed by the solution to the following equation:

$$Z_D(\omega_0, V_{RF}, I_{dc}) + Z_C(\omega_0, V_B) = 0 \tag{1}$$

where

- Z_D the IMPATT-diode impedance (Ω);
- Z_C the circuit impedance (Ω);
- ω_0 the oscillator frequency (rad/s);
- V_{RF} the diode RF voltage (V);
- I_{dc} the diode bias current (mA);
- V_B the varactor bias voltage (V).

The VCO performance with respect to tuning bandwidth and power output may be analyzed as a function of diode and circuit parameters from the solution of this equation. However, due to the complexity of the equivalent circuits of both Z_D and Z_C, this cannot be solved in closed form but must be solved by an iterative technique at each operating point. This section of the short paper discusses the models for both of the impedances Z_D and Z_C, and presents results of a computer program which solves (1) at each operating point.

For the large-signal characterization of the IMPATT diode, a simple Read-diode model was incorporated [8],[9]. For a given dc bias current, the small-signal impedance of a typical IMPATT diode as calculated by this program is shown in Fig. 1 on the extended Smith chart. The large-signal model was used to generate a matrix of impedances as a function of frequency and RF voltage. This impedance matrix represents the impedance function Z_D in (1).

Since Z_C must be the negative of Z_D from (1), the frequency dependence of Z_C can be deduced from a plot of $-Z_D$, as is also shown in Fig. 1 for the small-signal impedance case. This figure

Manuscript received October 21, 1974; revised January 9, 1975.
D. H. Claxton is with TRW Systems, Redondo Beach, Calif.
P. T. Greiling is with the Department of Electrical Sciences and Engineering, University of California, Los Angeles, Calif. 90024.

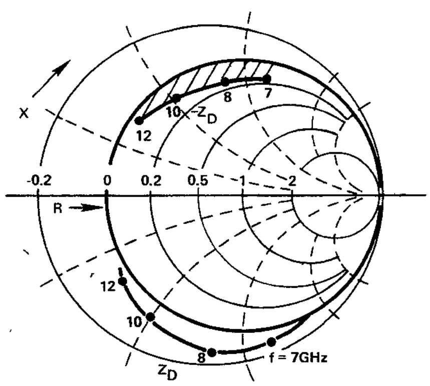

Fig. 1. Smith chart plot of small-signal impedance of IMPATT diode.

shows the manner in which the circuit must behave as a function of frequency in order to achieve broad-band tuning. The circuit's impedance plot must pass through or outside of the curve as represented by the cross-hatched area. One fundamental difficulty is immediately apparent from this plot. Foster's Reactance Theorem [10] states that a plot of impedance versus frequency for any linear passive circuit will move in a generally clockwise direction on the Smith chart with increasing frequency. Since the circuit's impedance plot must move counterclockwise, the tuning range of the variable element must be great enough to overcome the natural effects of all the other circuit elements. The circuit chosen to do this is a varactor-tuned ridged waveguide circuit as shown schematically in Fig. 2.

The IMPATT diode is situated in the middle of a low impedance section of waveguide and has one varactor on either side of it, followed by a higher impedance section of waveguide and then a a transition from the waveguide to 50-Ω coaxial. The diodes are mounted in anodized aluminum to provide dc isolation.

The main difficulty in the design of either wide-band microwave diode amplifiers or oscillators is that the magnitude of the diode impedance is typically low and decreases with frequency, whereas the transmission-line impedance to which the diode must be matched is normally much larger and independent of frequency (i.e., 50-Ω coaxial). The magnitude of the impedance of the transmission line can be scaled to match that of the IMPATT diode at one frequency by selection of the proper dimensions for the line. One of the unique features of this design is the choice of an impedance-matching technique which eases the difficulty of matching the impedance over a wide band. The basis for this technique can be understood from the impedance plots in Fig. 3. The plotted IMPATT impedance has been approximated by the magnitude of the reactance of its depletion-layer capacitance. In order to match the diode over a broad frequency range, the waveguide or TEM impedances must be altered by a tuning element to match that of the IMPATT diode. Because of the frequency variation of the waveguide impedance, the necessary compensation of the tuning element is much less than for the case of the TEM impedance. This means that for a given frequency change, less of the tuning element's variation is required to rematch the diode and the waveguide at the new frequency. That is, a smaller varactor variation is required to affect a given frequency change, or given a total varactor range, a wider range of frequencies can be tuned in the waveguide line than in the TEM line. Computer experiments indicate that in circuits which are similar in every way except for the type of transmission line used, waveguide tuning can offer a two to three times improvement over TEM line tuning. The reasons for using a ridged guide instead of a rectangular waveguide are because of the broad single-mode bandwidth possible, because of the ease of constructing low-impedance guide, and because of its compact size. The broad single-mode bandwidths mean that diodes can be placed closer together with less danger of evanescent mode coupling, which is proportional to the ratio of the operating frequency to the cutoff frequency of the evanescent mode. In a ridged guide the cutoff frequency of the second mode can be made

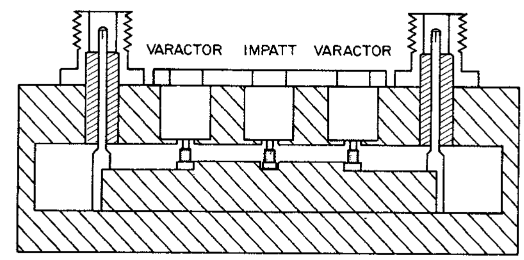

Fig. 2. Ridged waveguide IMPATT-diode VCO.

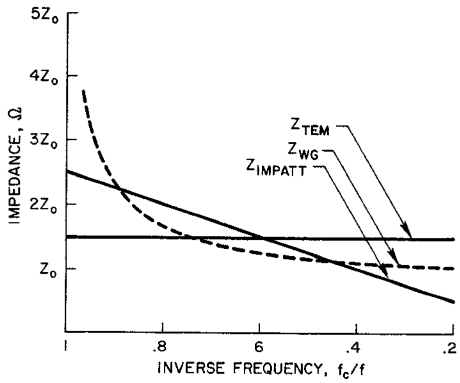

Fig. 3. Normalized waveguide, TEM, and IMPATT impedance variation with frequency.

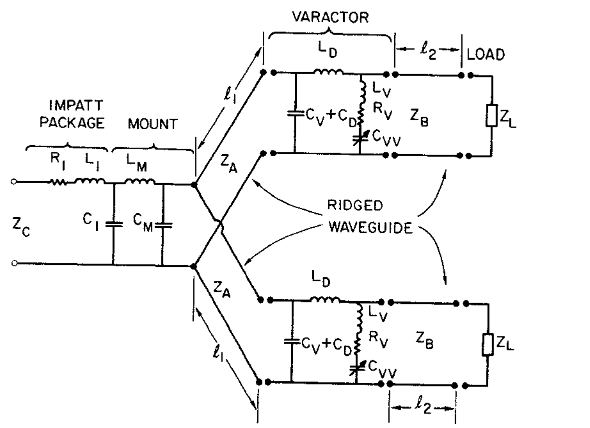

Fig. 4. IMPATT-diode VCO equivalent circuit. Z_C is impedance presented to IMPATT chip. R_l is IMPATT series resistance. L_l is IMPATT package lead inductance. C_l is IMPATT package capacitance. L_M is IMPATT mount inductance. C_M is IMPATT mount capacitance. Z_A,Z_B are waveguide impedances. l_1,l_2 are lengths of waveguide sections. L_D is discontinuity inductance. C_D is discontinuity capacitance. C_V is varactor package capacitance. L_V is varactor package inductance. R_V is varactor series resistance. C_{VV} is variable-varactor capacitance. Z_L is load impedance.

three to five times higher than that of the first mode, whereas in a rectangular guide it is only twice that of the first mode.

Fig. 4 shows the circuit model for the varactor-loaded ridged waveguide circuit which is a combination of lumped elements, distributed elements, and transmission lines.

Another unique feature of the circuit is the use of two varactors, one on each side of the IMPATT diode. Behind the varactors the ridged guide is matched into two 50-Ω coaxial lines [11],[12]. This eliminates the inherently narrow-band behavior which results from having a short located behind the IMPATT diode.

The two outputs can be combined externally if desired, but there are several applications for which two VCO outputs are useful. For example, if one employs a dual-conversion scheme in the receiver front end, the same VCO could be used for two receivers operating at different signal frequencies. Or, if a phase-lock receiver is envisioned, one VCO output would be in the phase-lock loop while the other would be used to mix or demodulate the signal.

The basic operation of this circuit can be understood as follows. First, because of the symmetry about the IMPATT diode, we can just examine one-half of the circuit. The section from the varactor diode to the IMPATT diode is, in effect, a quarter-wave transformer since $Z_B > Z_A$ and $l_1 \sim (\lambda/4)$ at the center frequency of the desired tuning range. This helps to give the desired small real part of the impedance seen by the diode. The inductive reactance is achieved by placing the varactor some distance from the diode so that its impedance (which is made somewhat less capacitive by its lead inductance) actually looks like that of a variable inductor.

In order to calculate qualitatively how the circuit should behave, the element values in the equivalent circuit in Fig. 4 were determined experimentally. The diode and varactor packages, which were the same style, and the varactor capacitance and series resistance were characterized in a 7-mm coaxial test fixture by conventional methods [13]. The mount and discontinuity elements were obtained experimentally by making impedance measurements from the IMPATT-diode position via a diode-package test fixture. A diode package was drilled out and a small coaxial line (0.032-in OD) was inserted into the base. The center conductor protruded ~ 0.005 in and had a #38 wire soldered from it to the top edges of the diode package. This was inserted into the circuit where the IMPATT diode would normally be placed. Then the network analyzer was used to measure directly the impedance that is presented to the diode chip. The element values C_M and L_M were determined by correlating measured impedance data and calculated impedance with C_M and L_M as parameters. The impedance measurements were taken with the test fixture in a simplified ridged waveguide circuit (no varactors) in which short circuits could be placed at several locations. The discontinuity elements C_D and L_D were determined in a similar manner by correlating measured and calculated impedances with C_D and L_D as parameters.

A computer program was incorporated which calculates the value of Z_C as a function of frequency, varactor bias, and circuit-element values and locates the operating point of the oscillator by matching to the negative of the diode impedance matrix. This program was used to design the circuit to yield the broadest tuning range. A typical circuit and diode impedance response as obtained by the program is shown in Fig. 5 on the G–B plane. For this particular case, the predicted bandwidth over which the diode will oscillate is 40 percent with a 20-dB power variation.

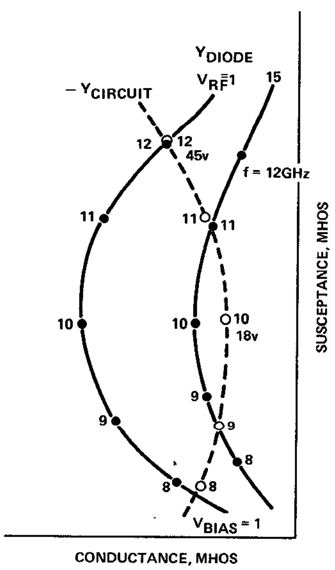

Fig. 5. Admittance of IMPATT diode and circuit as a function of frequency, RF voltage, and varactor bias voltage.

III. EXPERIMENTAL RESULTS

The ridged waveguide circuit shown in Fig. 2 was designed by the computer optimization program. The IMPATT, varactor diode, and package parameters were held constant while the total tuning range was optimized as a function of the diode mount and waveguide parameters. In particular, the variables $C_M, L_M, l_1, l_2, Z_A, Z_B$, and the waveguide cutoff frequency were optimized. The VCO circuit is shown in Fig. 6. The IMPATT diodes were Raytheon MS805A's with a nominal output of 500 mW. The varactor diodes were MA45102 Si tuning diodes with a Q of 2500 at 50 MHz.

The VCO performance is summarized in Figs. 7 and 8 in which oscillator frequency, power output, and efficiency are plotted as a function of the varactor bias. These results correspond to a total tuning range of 27.4 percent centered at 8.285 GHz with a ±3-dB power variation. The VCO was operated with one output connected to a power meter and with the other output through a frequency meter to a spectrum analyzer. Secondary oscillations of two types were observed occasionally at some varactor biases. Nonharmonically related oscillations were present around 12 GHz. These were at least 35 dB below the primary output. The second harmonic was also detectable, always at least 50 dB below the fundamental. The wave-

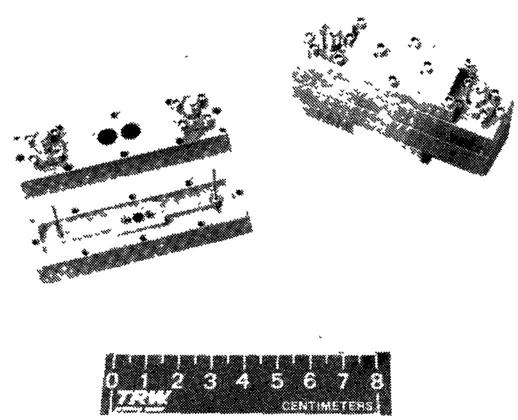

Fig. 6. IMPATT-diode VCO circuit.

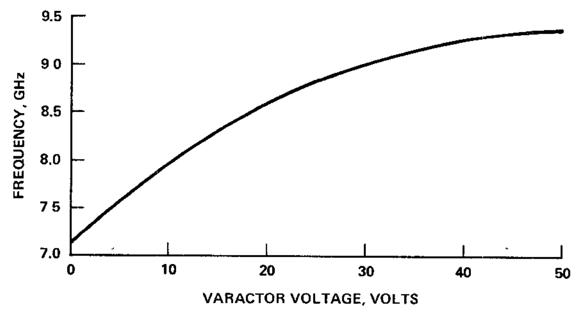

Fig. 7. Frequency versus varactor bias voltage.

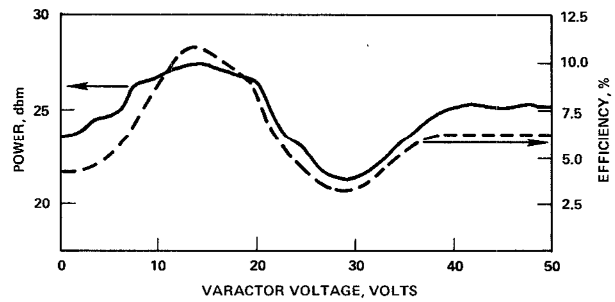

Fig. 8. Power output and efficiency versus varactor bias voltage.

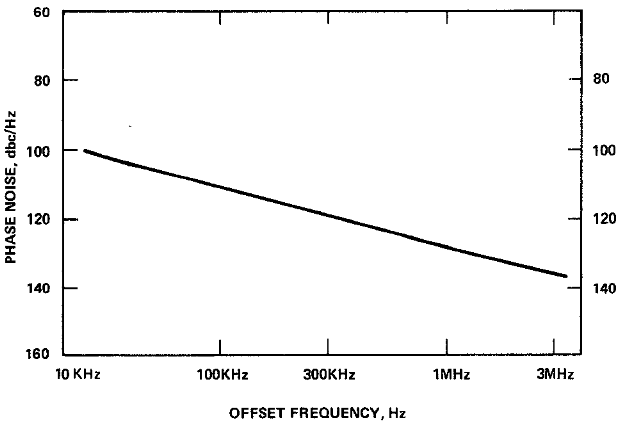

Fig. 9. FM noise versus offset frequency.

guide and the coaxial-to-waveguide transition tend to act as a bandpass filter, helping to reduce these out-of-band oscillations.

The VCO was also operated with a short in place of one of the varactors. The tuning bandwidth for this higher Q circuit was less than one-half of the two-varactor circuit due to the inherently narrow-band nature of the short behind the IMPATT diode.

The VCO noise performance ultimately determines the receiver front-end sensitivity and the amount of processing (and thus, hardware) required in the back end. The phase noise was measured in a test setup which uses klystrons as a reference and which has a sensitivity of at least 150 dBc/Hz. The noise performance is plotted in Fig. 9. This result is 8–10 dB better than previously reported for wide-band varactor-tuned VCO's, and would be considered more than adequate for most VCO applications.

IV. CONCLUSIONS

A varactor-tuned IMPATT-diode oscillator with 27-percent tuning bandwidth in X band has been achieved with inexpensive, commercially available IMPATT and varactor diodes. The equivalent-circuit model of the VCO predicts for higher power IMPATT's (i.e., larger negative conductances) and higher Q varactors, total tuning ranges in excess of 40 percent in X band. These tuning ranges have been obtained with reasonable tuning linearity and without significant sacrifice in power output or efficiency. Also the noise performance of the oscillator has not been degraded.

REFERENCES

[1] R. F. Soohoo, *Microwave Electronics* (Engineering Series). Menlo Park, Calif.: Addison-Wesley, 1971, pp. 184–206.

[2] G. I. Haddad, P. T. Greiling, and W. E. Schroeder, "Basic principles and properties of avalanche transit-time devices," *IEEE Trans Microwave Theory Tech.* (*Special Issue on Microwave Circuit Aspects of Avalanche-Diode and Transferred Electron Devices*), vol. MTT-18, pp. 752–772, Nov. 1970.

[3] N. S. Chang, T. Hayamizu, and Y. Matsuo, "YIG-tuned Gunn effect oscillator," *Proc. IEEE* (Lett.), vol. 55, p. 1621, Sept. 1967.

[4] B. Glance, "A magnetically tunable microstrip IMPATT oscillator," *IEEE Trans. Microwave Theory Tech.* (Short Papers), vol. MTT-21, pp. 425–426, June 1973.

[5] M. I. Grace, "Varactor-tuned avalanche transit-time oscillator with linear tuning characteristics," *IEEE Trans. Microwave Theory Tech.* (Corresp.), vol. MTT-18, pp. 44–45, Jan. 1970.

[6] ——, "Magnetically tunable transit-time oscillator," *Proc. IEEE* (Lett.), vol. 56, pp. 771–773, Apr. 1968.

[7] P. T. Greiling, P. Goodman, and G. I. Haddad, "Varactor-tuned avalanche diode oscillators in microstrip," Omni Spectra Tech. Rep., Feb. 1971.

[8] W. E. Schroeder and G. I. Haddad, "Effect of harmonic and subharmonic signals on avalanche-diode oscillator performance," *IEEE Trans. Micowave Theory Tech.* (Corresp.), vol. MTT-18, pp. 327–331, June 1970.

[9] W. E. Schroeder, P. T. Greiling, and G. I. Haddad, "Multifrequency operation of IMPATT diodes," presented at the Int. Electron Devices Meeting, Washington, D. C., Oct. 29–31, 1969.

[10] S. Ramo, J. R. Whinnery, and T. Van Duzer, *Fields and Waves in Communications Electronics.* New York: Wiley, p. 614, 1965.

[11] S. B. Cohn, "Properties of ridge wave guide," *Proc. IRE*, vol. 35, pp. 783–788, Aug. 1947.

[12] ——, "Design of simple broad-band wave-guide-to-coaxial-line junctions," *Proc. IRE*, vol. 35, pp. 920–926, Sept. 1947.

[13] P. T. Greiling and R. W. Laton, "Determination of semiconductor junction device package networks," *IEEE Trans. Microwave Theory Tech.* (*Part II of Two Parts—1974 Symposium Issue*), vol. MTT-22, pp. 1140–1146, Dec. 1974.

X-Band Microstrip-Inserted Puck Circulator Using Arc-Plasma-Sprayed Ferrite

Y. S. WU, MEMBER, IEEE,
F. J. ROSENBAUM, SENIOR MEMBER, IEEE, AND
D. H. HARRIS, MEMBER, IEEE

***Abstract*—Experimental circulators using ferrite pucks which have been sprayed into cavities in dielectric substrates by an arc-plasma-spray (APS) process are described.**

Microwave-quality ferrite materials can be quickly and efficiently deposited using the arc-plasma-spray (APS) process [1],[2]. This short paper reports on the performance of two X-band microstrip circulators fabricated with Trans-Tech TT1-105 ferrite deposited in a circular hole of diameter 0.195 in, in a 0.035-in-thick dielectric substrate whose relative dielectric constant is $\epsilon_d = 13$. The blind holes were ultrasonically cut in the substrate to a depth of 0.025 in or less. After deposition, the samples were lapped such that the final substrate thickness was 0.025 in, and the ferrite thickness was 0.020 in. The substrate dimensions are 1 in $\times$ 0.5 in nominal. Table I compares the properties of sintered-bulk TT1-105 with those of APS TT1-105. A photograph of a representative circulator and a sample substrate is shown in Fig. 1.

TABLE I
COMPARISON OF BULK PROPERTIES OF TT1-105 WITH THOSE OF APS TT1-105

Property	Bulk*	APS**
Saturation Magnetization $4\pi M_s$	1750	1750
Coercivity, H_c (Oe)	1.16	1.1
Remanence Ratio, M_r/M_s	70%	80%
Gyromagnetic Resonance Measurements at 9.4 GHz		
Average 3 dB linewidth, ΔH (Oe)	225	112
Average g-effective	1.98	---
Permittivity Measurements at 9.4 GHz		
Average Dielectric Constant, ε'	12.2	12.2
Average Loss Tangent, $\tan\delta$	<.00025	<.0002
Density > 99% of Theoretical		

* Trans. Tech. Catalog.
** Measured.

Manuscript received August 1, 1974; revised January 20, 1975. This work was supported by the Air Force Avionics Laboratory under Contract F33615-72-C-1034.

Y. S. Wu was with the Department of Electrical Engineering, Washington University, St. Louis, Mo. 63130. He is now with the Central Research Laboratory, Texas Instruments Incorporated, Dallas, Tex. 75222.

F. J. Rosenbaum is with the Department of Electrical Engineering, Washington University, St. Louis, Mo. 63130.

D. H. Harris is with Monsanto Research Corporation, Dayton, Ohio 45407.